Available online at www.easdprocedia.org
EASD Procedia EURODYN (2020) 936-947

EASD Procedia

EURODYN 2020
XI International Conference on Structural Dynamics
M. Papadrakakis, M. Fragiadakis, C. Papadimitriou (eds.)
Athens, Greece, 23–26 November 2020

INVESTIGATION ON DAMAGE SENSITIVE FEATURES FOR OPTIMAL SENSOR NETWORKS BASED ON REAL-SCALE RECORDINGS

Said Quqa[1], Michelangelo Maria Malatesta[1], Panagiotis Martakis[2], Artur Movsessian[3]

[1]University of Bologna
Department of Civil, Chemical, Environmental and Materials Engineering / Advanced Research Center on Electronic Systems
Viale del Risorgimento 2, 40136 / Viale Carlo Pepoli 3/2, 40123 Bologna
e-mail: {said.quqa2,michelange.malatest2}@unibo.it

[2] ETH Zurich
Chair of Structural Mechanics and Monitoring
Stefano-Franscini-Platz 5, CH-8093, Zurich
e-mail: martakis@ibk.baug.ethz.ch

[3] University of Edinburgh
School of Engineering, Institute for Infrastructure and Environment
Alexander Graham Bell Building, Thomas Bayes Road, Edinburgh EH9 3FG, United Kingdom
e-mail: Artur.Movsessian@ed.ac.uk

Keywords: Damage Sensitive Features, Optimal Sensor Networks, Structural Health Monitoring

Abstract. *Structural health monitoring (SHM) includes a wide range of methods focusing on the improvement of structural reliability and life cycle management of engineered systems. In the past decades, smart maintenance procedures have been proposed and implemented for a large number of civil structures with strategic and monumental relevance. Nowadays, rapid advances in signal processing and sensor technology allow for the implementation of smart maintenance schemes for conventional buildings and infrastructure. Vibration-based SHM techniques are among the most applied in the structural engineering field and become increasingly popular due to their interdisciplinary nature. In this framework, the establishment of reliable damage-sensitive features (DSF) is crucial for the efficient evaluation of structural health. This work comprises an investigation on the effectiveness of data-driven DSFs for the case of a large scale reinforced concrete benchmark under shaking table excitation. Different damage identification techniques are applied to expose the propagation of structural damage during strong ground motions. A discussion on the hardware and algorithmic requirements for reliable wireless smart sensor networks (WSSNs), capable of capturing the desired DSFs, is also included.*

ISSN:2311-9020
Peer-review under responsibility of the Organizing Committee of EURODYN 2020.
doi: 10.47964/1120.9074.19628

1 INTRODUCTION

Despite the unavoidable costs for installation and supervision, the information obtained through monitoring proves to be invaluable in the aftermath of catastrophic events. The recent disaster of the Morandi bridge exposed the unexploited potential of measurements for the maintenance of aging structures. Considerations regarding the life cycle management consist today a prime part of the design of major infrastructure facilities. Structural health monitoring (SHM) provides the tools and the methodologies that allow for the optimization of the maintenance activities along the operational life of structures with substantial impact on the life cycle costs and the safety of the public.

Rapid advances in hardware and software capabilities allow for the widespread diffusion of SHM techniques in the conventional building stock [1, 2]. In particular, Wireless Smart Sensor Network (WSSNs) are the most promising systems for SHM applications because they don't require long cables leading a significant cost reduction and an easier installation procedure. Moreover, WSSNs are characterized by low cost and feature edge-computing capabilities enabling the decentralization of the monitoring process, by reducing the amount of data transferred and improving the energy efficiency of the monitoring configuration [3]. The energy consumption of a wireless network dictates the maintenance intervals and thus consists the bottleneck for the optimal design of WSSNs. Given that energy consumption is highly related to the network architecture, the choice of a suitable network topology for the studied application is of major importance. Shrestha and Xing [4] discussed the performance of various WSSNs topologies by comparing the reliability, energy–efficiency, network life, scalability, self-organizing capability and data latency. Other parameters that constrain further the design of optimal WSSNs stem from cost and size restrictions.

The recent paradigm of Internet of Things (IoT) [5] allows researchers to vision the Internet of STructures (IoST), where proper indexes could provide information regarding structural health at an urban scale, almost in real time. This information could support substantially both the vulnerability assessment as well as the post earthquake damage estimation, which is currently based on time consuming and inevitably subjective inspections. Despite extensive research in this field, the extraction of robust damage sensitive features (DSFs) from vibrational response still poses challenges, particularly related to damage characterization (location, severity) [6, 7]. A large category of DSFs focuses on changes of the modal properties due to structural damage. Noh and coworkers [8] proposed a DSF criterion, which relies on the ratio of the energy allocated on the first mode over the total energy of the response signal. Other candidate methodologies rely on changes in coherence between different nodes, the wavelet decomposition, Hilbert-Huang transform [9], higher order moments or entropy. Recently, Hwang and Lignos [10] described a framework for estimating story-based engineering demand parameters in instrumented steel frame buildings with steel moment-resisting frames. The proposed framework utilizes wavelet-based damage sensitive features and basic building geometric information to infer the building damage state at a given seismic intensity.

This work comprises the implementation of a wide palette of DSFs for the damage detection of full scale recordings. In section 2, the selected features are presented and the key parameters are described. In section 3, the selected features are applied for the evaluation of the recordings of a 7-storey shear wall benchmark experiment. In section 4 are summarized the results and the comparison of the performance of the studied DSFs. Finally, section 5 includes a discussion on the key issues for the design of a decentralised wireless sensor network in a SHM framework.

2 VIBRATION-BASED DAMAGE IDENTIFICATION

In this section, a brief description and some implementation examples of the selected DSFs are reported. Both modal– and non–modal–based features have been selected. In particular, autoregressive (AR) parameters and principal component analysis (PCA) of the covariance of raw acceleration data are usually referred as non–modal–based methods, as the identified parameters cannot be directly interpreted into a modal or physical domain. On the other hand, the curvature of uniform load lines (ULLs) obtained through the flexibility matrix and the transmissibility function belong to the family of modal–based DSFs. Relevant notions for novelty detection as well as damage indices (DIs) implemented in this study are also reported.

2.1 Autoregressive parameters

Autoregressive (AR) models are among the most popular non–modal–based structural identification tools. It has been shown that, despite the non–intuitive physical interpretation of AR parameters, the features captured by AR models, directly fitted to raw acceleration data, are representative of the structural behavior and can be analyzed to detect changes due to damage or changing environmental conditions [11]. AR parameters are computed following the assumption that each sample of a time series depends linearly on the previous samples and can be reconstructed by adding a residual term, which is usually assumed as Gaussian white noise. After selecting a model order (*i.e.*, how many samples are considered in the description of each element of the time series), the identification of AR parameters can be achieved through solving an ordinary least square problem. The simplicity of this method allowed for various implementation in SHM algorithms, involving different usage of AR parameters for the estimation of structural damage [12, 13].

2.2 Covariance–based DSF

Covariance is a common statistical feature that describes the relationship between two signals in time domain. Assessing the covariance of the vibrational responses of sensors placed in different position along a structure has been established as a valid statistical metric for capturing novelties in the dynamic response [14]. These changes, however, can be attributed not only to structural degradation, but also to changing environmental conditions [15]. Principal component analysis (PCA) [16] has been widely applied to enhance the novelty detection by a consequent algorithm. PCA is a linear transformation which is applied to a potentially correlated feature-set. The principal components (PCs) are sorted by their eigenvalues in a decreasing order, where the first PC has the highest explained variance after the transformation. This procedure can reduce the dimension of the feature-set while maintaining a high remaining variance explained.

2.3 Curvature of the uniform load line

Changes in modal curvature is the basis of various modal-based DSFs in the field of damage identification, as it is proven to be particularly effective to localize structural degradation related to stiffness reduction [17]. Major drawbacks of this this feature include its rather approximate computational scheme (i.e., the central difference method), starting from displacement lines, and the fact that at least three data points are required to evaluate each curvature value. As a result, modal curvature based DSFs tend to be too sensitive to inaccuracies in the identification of modal shapes and require a considerable amount of sensors, placed at equidistant locations.

In this paper, the curvature of the uniform load line (ULL) has been applied. This approach describes the structural behavior in the physical space and is less sensitive to identification errors for higher modal shapes [18]. In particular, the ULL of a structure represents the deflection shape under the application of a uniform load vector, the entries of which are unitary forces applied at each sensor location. The ULL is generally evaluated through the flexibility matrix of the structure **F**, which can be estimated by the first r vibration modes, as following:

$$\mathbf{F} \cong \sum_{j=1}^{r} \frac{1}{\omega_j^2} \mathbf{\Phi}_j \mathbf{\Phi}_j^T \tag{1}$$

where ω_j and $\mathbf{\Phi_j}$ indicate the j–th natural circular frequency and modal shape, respectively. The ULL can thus be computed as:

$$\mathbf{u} = \mathbf{Fp} \tag{2}$$

where $\mathbf{p} = [1, 1, \ldots, 1]^T$ has the same size as $\mathbf{\Phi}_j$.

It should be noted that, in order to compute the real flexibility matrix, modal shapes must be mass-normalized. In this case, a variation of **u** registered during a monitoring process could also be related to a physical quantification of damage in terms of flexibility increment (*i.e.*, stiffness decrement). In real case studies, however, there is often no precise information regarding the mass distribution, especially for complex structures. As a result, the evaluation of **F** becomes particularly challenging. For the purposes of the present work, a uniform distribution of masses along the height of the building is considered. This assumption coincides with the regular geometry of the studied benchmark experiment. Therefore, modal shapes are normalized with respect to an identity matrix, and **F** is considered as proportional to the real flexibility matrix. In this case, a quantification of damage in absolute terms is not possible, but the method still allows for the localization of damage [19].

2.4 Transmissibility based criteria

Transmissibility based criteria have been recently proposed in an attempt to detect and localize damage based on output-only data [20]. The transmissibility function between points *a* and *b* of an elastic system can be defined as the ratio of the complex amplitude of the system responses in frequency domain, which can be expressed as a fraction of power spectral densities:

$$T_{a,b}(\omega) = \frac{X_a(\omega) \times X_b(\omega)}{X_b(\omega) \times X_b(\omega)} = \frac{G_{a,b}(\omega)}{G_{b,b}(\omega)} \tag{3}$$

By implementing Pearson's correlation coefficient for the transmissibility vectors in different damage states, researchers defined a correlation-based damage indicator (CDI):

$$CDI_{a,b} = |\frac{Cov(T^d, T^u)}{\sigma_{T^d}\sigma_{T^d}}| \tag{4}$$

An additional feature based on the modal assurance criterion was also defined as transmissibility assurance criterion (TAC):

$$TAC_{a,b} = \frac{[(T^d)^T(T^u)]^2}{[(T^d)^T(T^d)][(T^u)^T(T^u)]} \tag{5}$$

where T^d and T^u represent the transmissibility vectors under damaged and healthy conditions. Considering the points *a* and *b* as the recording points along subsequent storeys of a building, transmissibility based criteria provide information for structural changes between the measuring points. For shear wall concrete buildings with rigid slabs, the earthquake induced damage is expected to concentrate in the lower floor levels. For such cases, transmissibility based criteria for damage detection and localisation are well defined. However, such criteria cannot provide robust estimation for the level of damage since they rely exclusively on low amplitude measurements, where the system is expected to respond in the equivalent elastic regime.

2.5 Mahalanobis Distance

The Mahalanobis distance (MD) is a widely applied multivariate distance metric to highlight novelties or outliers in a feature-set [21]. The MD measures the distance between a point and a distribution. The distribution is commonly calculated for a reference feature-set which is also called the training-set. The MD is described as follows:

$$d(\mathbf{x}^k, \mathbf{Y}) = \sqrt{(\mathbf{x}^k - \boldsymbol{\mu}_{\mathbf{Y}})^T \boldsymbol{\Sigma}_{\mathbf{Y}}^{-1} (\mathbf{x}^k - \boldsymbol{\mu}_{\mathbf{Y}})} \tag{6}$$

where $d(\mathbf{x}^k, \mathbf{Y})$ is the distance between a feature vector $\mathbf{x}^k$ and a reference $\mathbf{Y}$, with k being the k^{th} feature vector in a feature-set. $\boldsymbol{\mu}$ is the mean of features in $\mathbf{Y}$ and $\boldsymbol{\Sigma}$ the covariance of the reference feature-set. This metric is used as DI for the modal-based DSFs investigated in this work.

2.6 Damage indices and novelty detection

For most of the damage identification algorithms the identified parameters are compared to baseline information obtained right after the installation of the monitoring system. This baseline information is considered to represent the undamaged condition. To quantify this comparison, a proper DI has to be selected and a threshold between "damaged" and "healthy" state has to be defined. For the AR and covariance based DSFs the MD has been used as a DI since a statistically significant set of results were evaluated. For the former case, a different set of AR parameters can be identified for each data array (i.e., considering data intervals of user-defined length at each sensor location). In general, damage localization cannot be directly achieved by analyzing local modifications in AR parameters [13]. For this reason, the mean of MDs computed over the set of all recording nodes has been selected as the final DI for the purposes of damage detection. Similarly, the MD-based damage index is evaluated for the covariance and PCA based DSF. A threshold is selected for the reference state and is represented by T_{th}. The choice of T_{th} is based on a cumulative distribution of the damage index where the k^{th} percentile of the data is allowed to exceed the threshold. Consequently, $d(\mathbf{x}^k, \mathbf{Y}) > T_{th}$ are considered as novelties and are potentially correlated to damage.

For the modal-based DSFs longer datasets are required and thus only deterministic DIs can be defined through the analyzed data. For the curvature of the ULL, the percentage variation between local estimates of the DSF in different damage scenarios is considered. For the transmissibility based DSF the identified CDI and TAC metrics are evaluated.

3 DAMAGE DETECTION ON REAL-SCALE RECORDINGS

The DSFs described in Section 2 are evaluated using the data collected during a benchmark experiment on a full-scale RC structure tested on a shaking table at the University of California, San Diego [22, 23]. After a brief description of the case study, the results are reported and discussed.

(a)

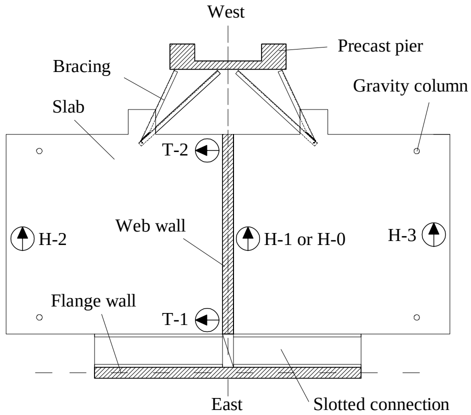

(b)

Figure 1: Picture of the tested structure (a) and ground floor plan of typical storey (b)

3.1 Description of the case study

The specimen, shown in Figure 1a, consists of two perpendicular walls (web and flange wall) and a concrete slab at each storey–level, supported by four gravity columns and an auxiliary post–tensioned column that provides torsional stability to the system (Figure 1b). Shaking table tests were designed to progressively damage the building through the simulation of four historic earthquakes recorded in California, with increasing intensity. Before and after each shaking test, the response of the building was recorded under white noise (WN) excitation, with a root mean square (RMS) amplitude equal to $0.03\,\mathrm{g}$, and low amplitude ambient vibration (AV), as described in detail in [22, 23] and in Table 1. In particular, between tests S3.1 and S3.2, the bracing system between the slabs and the post–tensioned column was stiffened. The present work focuses exclusively on the acceleration response during the white noise excitation before and after the strong shaking events.

The instrumentation of the tested structure includes 45 uniaxial accelerometers: 29 measuring the longitudinal direction (three on each floor slab, one on the web wall at mid-height of each story, and one on the pedestal base), 14 measuring the transversal direction (2 on each floor slab), and 2 nodes measuring the vertical direction (at the base, on the pedestal). In this paper seven different sensor configurations are considered, as described in Table 2, with reference to Figure 1b. The original data are sampled at $240\,\mathrm{Hz}$ and are here downsampled at $100\,\mathrm{Hz}$. More details about the geometry and the instrumentation can be found in [22, 23].

Test	Description
S0	8min WN (0.03%g RMS) + 3min AV
EQ1	San Fernando earthquake, 1971, longitudinal component, Van Nuys station
S1	8min WN (0.03%g RMS) + 3min AV
EQ2	San Fernando earthquake, 1971, transversal component, Van Nuys station
S2	8min WN (0.03%g RMS) + 3min AV
EQ3	Northridge earthquake, 1994, longitudinal component, Woodland Hills Oxnard Boulevard station
S3.1	8min WN (0.03%g RMS) + 3min AV
S3.2	8min WN (0.03%g RMS) + 3min AV
EQ4	Northridge earthquake, 1994, $360°$, Sylmar Olive View Med
S4	8min WN (0.03%g RMS) + 3min AV

Table 1: Testing setup

Deployment layout	Description
H-0	SD on the web wall in the horizontal direction, at floor levels and mid-height of storeys
H-1	SD on the web wall in the horizontal direction, at floor levels
H-2	SD on the southern part of the slab in the horizontal direction
H-3	SD on the northern part of the slab in the horizontal direction
T-1	SD on the eastern part of the web wall in the transversal direction, at the floor levels
T-2	SD on the western part of the web wall in the transversal direction, at the floor levels
HT	All sensors described above

Table 2: Sensor deployment layouts

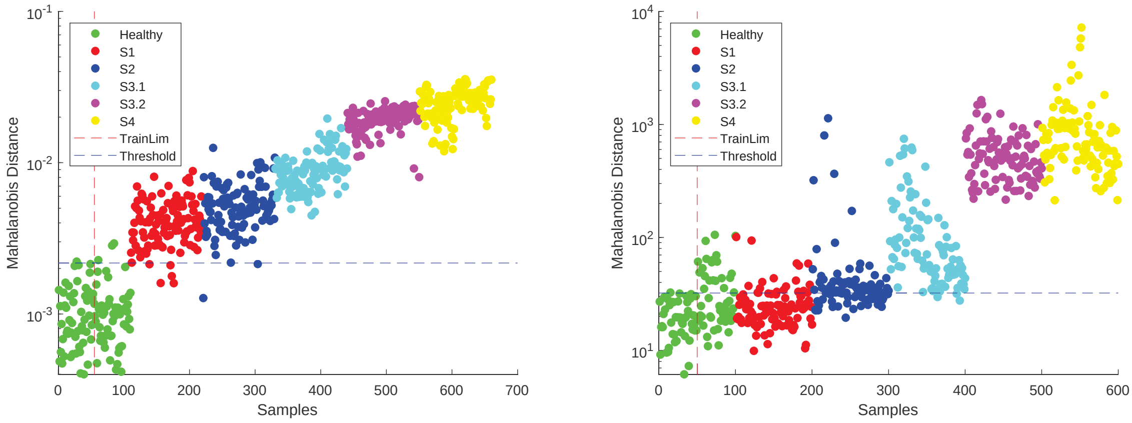

(a) AR Model

(b) Covariance based DSF

Figure 2: Control charts for non-modal-based DSFs

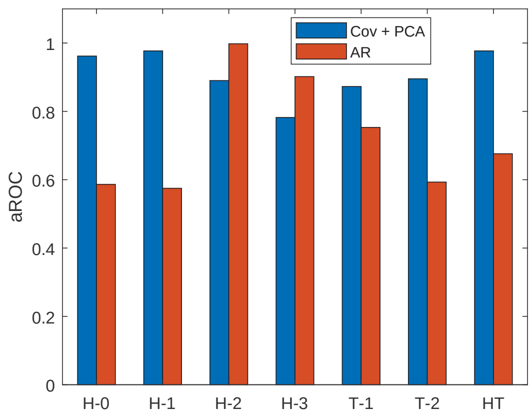

Figure 3: aROC and false alarm rates obtained for the non-modal-based approaches

3.2 Discussion of the results

For non-modal-based DSFs, a control chart approach demonstrates clearly the online novelty detection procedure for damage identification. Response windows of seven minutes, divided into sets of 1000-samples, are considered as separate inspection intervals. The DSF is computed for each inspection interval and compared to the baseline estimation, which is evaluated based on the first 55 intervals for condition S0. In Figure 2, the MD between the feature evaluation on each interval and the baseline is presented. For brevity, only the results for the sensor deployment layout T-1 are reported. The threshold for novelty detection is set in the training set and allows 1% of outliers. A comparison between the control charts of the AR based DSF (Figure 2a) and the covariance based DSF (Figure 2b) demonstrates that, the AR model captures adequately the transition from the healthy state to the first damaged state, while it fails to provide clear boundaries between the subsequent damage states. On the other hand, the covariance based DSF differentiates better significant damage (S4 and S5) from the initial damage states, while indicates minor variations from conditions S1 to S3.1.

Summary results obtained from the evaluation of these DSFs using all the deployment layouts of Table 2 are reported in Figure 3. It can be noticed that, although the false alarm rate of the covariance-based method is generally higher, the area under the ROC curve (indicated

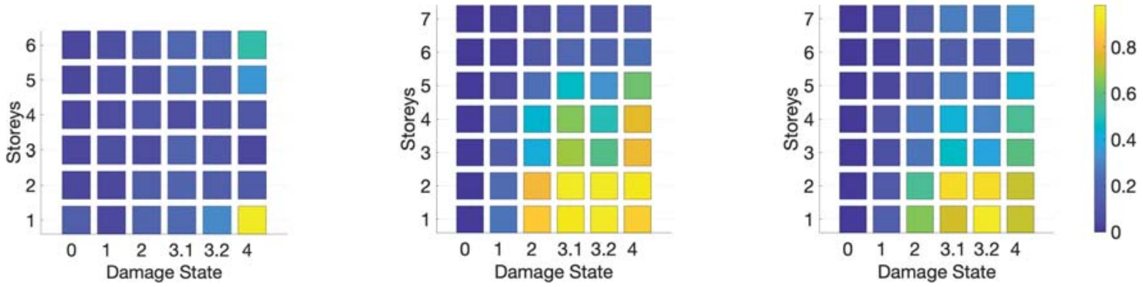

(a) Curvature (b) TAC (c) CDI

Figure 4: Transmissibility-based and curvature-based damage indices evaluated for each damage condition

here as aROC) is greater in most cases, denoting a better discrimination between healthy and damaged conditions. Moreover, it is worthy to note that the AR-based method works better in the transversal direction, showing higher aROC values, while the covariance-based approach performs well in all the deployment layouts.

Figures 4a, 4b and 4c illustrate the damage indices calculate by the curvature-based and the transmissibility based approaches, by considering the sensor deployments H-1. In this work, a deterministic comparison between healthy and damaged conditions is considered. In order to compute curvature, the central difference method is employed, assuming that the base displacement is 0, obtaining 6 curvature values.

While the curvature-based approach is less sensitive to small damages, the transmissibility function appears to detect also small variations in the dynamic behavior, showing an accurate estimation of the damage position and consistent representation of the identified damage degradation due to increasing the excitation amplitude. Moreover, the TAC criterion proves to be more sensitive to damage in comparison to the CDI criterion.

4 CONSIDERATIONS ON WIRELESS SENSOR NETWORK IMPLEMENTATIONS

The considerations reported in this section refer to a star-topology network. This is one of the most commonly used topology due to its simplicity, although Cluster Head and mesh topologies provide a better flexibility, *i.e* network scalability, communication reliability or energy management [4]. In particular, the network was designed to collect n samples of acceleration data at each node location at user-defined inspection intervals. Depending on the feature, DSFs are then partially or fully computed in the central monitoring station (*i.e.*, the sink node), where damage identification takes place. Table 3 summarizes the main characteristics of interest for the implementation of DSFs on a WSSN. While univariate AR parameters and covariance can only identify structural changes due to modifications of the dynamic response in time domain, modal-based parameters can provide information about the position and, under certain assumptions, the extent of damage. The number of channels needed to calculate each DSF reflects the possibility to compute it in a decentralized manner, by performing part of the processing on the nodes. The minimum number of samples to be transferred to the central monitoring station for the evaluation of the DSFs is also considered as a performance index.

AR parameters are identified on single data series, such as the raw acceleration signals recorded by each node. In this case, AR parameters could be identified onboard and the transmission could be reduced to the selected order of the AR model (p). Covariance and trans-

DSF	Id level	Num. of channels	Num. of samples	Complexity
AR parameters	Detection	$\geqslant 1$	p	O(p^2n)
Covariance	Detection	$\geqslant 2$	n	-
Curvature	Loc./Quant.	$\geqslant 3$	n	-
Transmissibility	Localization	$\geqslant 2$	s	O($slog(s)$)

Table 3: Characteristics of the considered DSFs

missibility functions require couples of acceleration channels for their evaluation in time and frequency domain respectively. Truncated spectra can thus be employed to estimate the transmissibility in the band of interest. The number of samples required at the level of central node is therefore equal to the number of points of the truncated frequency spectrum (s), which can be computed on each node before transmission. The curvature based DSF requires recordings of at least three subsequent nodes to be computed. Hence, the identification of this feature has to be performed in a centralized fashion with complete data series, in order to preserve phase information.

Computational complexity is an aspect of utmost importance when decentralized processes are implemented on low-cost smart nodes, since they are generally characterized by small computational capabilities and limited battery life. The identification of AR parameters can be obtained through several algorithms with varying complexity. The ordinary least squares problem yields an asymptotical complexity of O(p^2n), with p denoting the order of AR model and n the number of training samples. Alternatively, through the Yule-Walker method, the complexity becomes O($p^2 + np$), still being strongly dependent on the selected order, which increases with the structural complexity. Among the different Yule-Walker solvers, Dushin and Frolov [24] exploited the Levinson–Dusrbin recursion for extrapolating AR coefficients and monitoring environmental phenomena such as humidity and light. Lynch [25] exploited the Burg's method to solve the Yule-Walker equations which avoids complex matrix inversion operations. In such a case, considering 4000–time samples and the identification of 30 AR coefficients, the WSSN needed $8\,\mathrm{s}$ of computational time with $3\,\mathrm{J}$ of energy consumption.

Covariance and curvature based DSFs are not suitable for decentralization in a simple star-topology network. Hence, the computational complexity at the central node is high, involving the evaluation of all couples of covariance functions for the former feature, and a complete automated modal identification for the latter. The computation of the frequency spectrum for the identification of transmissibility functions can be conducted on the nodes with a complexity of O($slog(s)$), by implementing fast Fourier transform (FFT) with s frequency points. It is worth mentioning that Goertzel's algorithm [26] can also be utilized for frequency analysis with a computational complexity of O(s) for a single bin of the spectrum and exploiting recursion [27].

5 CONCLUSIONS

Despite recent advances in algorithms and hardware related to damage identification, SHM remains an unexploited potential in civil engineering practice. The substantial costs related to the instrumentation and the management of the recorded data undermine the widespread implementation of sensors networks that could provide valuable insights into the structural behaviour of infrastructure and buildings during and after catastrophic events. This work explores the efficiency of various modal-based and data-driven DSFs, implemented on real scale recordings. The applicability of the studied DSFs in low cost WSSNs, in terms of computational complexity, energy efficiency and data transmission, is also discussed.

In the present case, data-driven DSFs estimated by short data series detect accurately damage and could be computed almost in real time in permanent SHM applications. While the AR-based approach proves to be more robust in sensing the transition from healthy to damaged state, the covariance–based approach is more suitable to identify severe structural degradation. The possibility to compute the AR parameters on smart nodes allows for the decentralization of the processing, reducing substantially the volume of the data to be transmitted. For distributed sensor networks, modal–based DSFs can provide information related to both the location and the severity of damage. In the present study, transmissibility–based approaches perform very well in both tasks. Although these indexes can only be assessed in the central node, the required information reduces to truncated spectral coordinates. Finally, the curvature-based approach proves to be sensitive only to severe damage and is not suitable for decentralized configurations.

REFERENCES

[1] B.F. Spencer Jr, J-W. Park, K.A. Mechitov, H. Jo, and G Agha. Next generation wireless smart sensors toward sustainable civil infrastructure. *Procedia Engineering*, 171:5–13, 2017.

[2] F. Zonzini, M. M. Malatesta, D. Bogomolov, N. Testoni, L. De Marchi, and A. Marzani. Heterogeneous sensor-network for vibration-based shm. In *2019 IEEE International Symposium on Measurements & Networking (M&N)*, pages 1–5. IEEE, 2019.

[3] M. Abdulkarem, K. Samsudin, F. Z. Rokhani, and M. F. A Rasid. Wireless sensor network for structural health monitoring: A contemporary review of technologies, challenges, and future direction. *Structural Health Monitoring*, page 1475921719854528, 2019.

[4] A. Shrestha and L. Xing. A performance comparison of different topologies for wireless sensor networks. In *2007 IEEE Conference on Technologies for Homeland Security*, pages 280–285. IEEE, 2007.

[5] C. Scuro, P. F. Sciammarella, F. Lamonaca, R. S. Olivito, and D. L. Carni. Iot for structural health monitoring. *IEEE Instrumentation & Measurement Magazine*, 21(6):4–14, 2018.

[6] F. Casciati and S. Casciati. Structural health monitoring by Lyapunov exponents of non-linear time series. *Structural Control and Health Monitoring*, 13(1):132–146, 2006.

[7] P. Omenzetter and J.M.W. Brownjohn. Application of time series analysis for bridge monitoring. *Smart Materials and Structures*, 15(1):129–138, 2006.

[8] H. Young Noh, K. Krishnan Nair, D. G. Lignos, and A. S. Kiremidjian. Use of wavelet-based damage-sensitive features for structural damage diagnosis using strong motion data. *Journal of Structural Engineering*, 137(10):1215–1228, 2011.

[9] N.E. Huang, Z. Shen, S.R. Long, M.C. Wu, H.H. Snin, Q. Zheng, N.C. Yen, C.C. Tung, and H.H. Liu. The empirical mode decomposition and the Hubert spectrum for nonlinear and non-stationary time series analysis. *Proceedings of the Royal Society A: Mathematical, Physical and Engineering Sciences*, 454(1971):903–995, 1998.

[10] S. H. Hwang and D. G. Lignos. Nonmodel-based framework for rapid seismic risk and loss assessment of instrumented steel buildings. *Engineering Structures*, 156:417–432, 2018.

[11] H. Sohn, J.A. Czarnecki, and C.R. Farrar. Structural health monitoring using statistical process control. *Journal of structural engineering New York, N.Y.*, 126(11):1356–1363, 2000. cited By 280.

[12] R. Yao and S. N Pakzad. Autoregressive statistical pattern recognition algorithms for damage detection in civil structures. *Mechanical Systems and Signal Processing*, 31:355–368, 2012.

[13] G.M. Steven and M.P. Sudhakar. Statistical moments of autoregressive model residuals for damage localisation. *Mechanical Systems and Signal Processing*, 20(3):627 – 645, 2006.

[14] D. Tcherniak and L.L. Mølgaard. Vibration-based shm system: application to wind turbine blades. In *Journal of Physics: Conference Series*, volume 628, page 012072. IOP Publishing, 2015.

[15] D. Tcherniak and L.L. Mølgaard. Active vibration-based structural health monitoring system for wind turbine blade: Demonstration on an operating vestas v27 wind turbine. *Structural Health Monitoring*, 16(5):536–550, 2017.

[16] A.-M. Yan, G. Kerschen, P. De Boe, and J.-C. Golinval. Structural damage diagnosis under varying environmental conditions—part ii: local pca for non-linear cases. *Mechanical Systems and Signal Processing*, 19(4):865–880, 2005.

[17] W. Fan and P. Qiao. Vibration-based damage identification methods: A review and comparative study. *Structural Health Monitoring*, 10(1):83–111, 2011. cited By 1029.

[18] J. Wang and P. Qiao. Improved damage detection for beam-type structures using a uniform load surface. *Structural Health Monitoring*, 6(2):99–110, 2007.

[19] S. Quqa, L. Landi, and P.P. Diotallevi. Instantaneous modal identification under varying structural characteristics: A decentralized algorithm. *Mechanical Systems and Signal Processing*, 142:106750, 2020.

[20] Y.L. Zhou, H. Cao, Q. Liu, and M.A. Wahab. Output-based structural damage detection by using correlation analysis together with transmissibility. *Materials*, 10(8):1–17, 2017.

[21] H. Sohn, C.R. Farrar, N.F. Hunter, and K. Worden. Structural health monitoring using statistical pattern recognition techniques. *J. Dyn. Sys., Meas., Control*, 123(4):706–711, 2001.

[22] B. Moaveni, X. He, J.P. Conte, and J.I. Restrepo. Damage identification study of a seven-story full-scale building slice tested on the ucsd-nees shake table. *Structural Safety*, 32(5):347–356, 2010.

[23] B. Moaveni, X. He, J. P. Conte, J. I Restrepo, and M. Panagiotou. System identification study of a 7-story full-scale building slice tested on the ucsd-nees shake table. *Journal of Structural Engineering*, 137(6):705–717, 2011.

[24] S.V. Dushin and S.A. Frolov. Distributed data compression algorithm for low-power wide-area networks. In *International Conference on Distributed Computer and Communication Networks*, pages 163–173. Springer, 2019.

[25] J.P. Lynch, A. Sundararajan, K.H. Law, A.S. Kiremidjian, and E. Carryer. Embedding damage detection algorithms in a wireless sensing unit for operational power efficiency. *Smart Materials and Structures*, 13(4):800, 2004.

[26] G. Goertzel. An algorithm for the evaluation of finite trigonometric series. *The American Mathematical Monthly*, 65(1):34–35, 1958.

[27] M. Bocca, J. Toivola, L. M. Eriksson, J. Hollmén, and H. Koivo. Structural health monitoring in wireless sensor networks by the embedded goertzel algorithm. In *2011 IEEE/ACM Second International Conference on Cyber-Physical Systems*, pages 206–214. IEEE, 2011.